Macromolecules
COMMUNICATION TO THE EDITOR

Macromolecules **2010**, *43*, 5521–5523 **5521**
DOI: 10.1021/ma100799s

Investigation of Reactive Polymer−Polymer Interface Using Nanomechanical Mapping

Dong Wang,* So Fujinami, Hao Liu, Ken Nakajima, and Toshio Nishi

WPI Advanced Institute for Materials Research, Tohoku University, 2-1-1 Katahira, Aoba, Sendai 980-8577, Japan

Received April 13, 2010
Revised Manuscript Received May 24, 2010

Achieving compatibilization of immiscible polymer blends is a convenient and attractive way for obtaining high-performance polymeric materials.[1,2] For this purpose the following two methods are usually used: one is the addition of premade block or graft copolymer during mixing of the immiscible blends, and the other is reactive compatibilization in which the block or graft copolymer is formed in situ at the interfacial regions. The preadded or in situ formed copolymer is believed to play the role of an emulsifier, which promotes compatibilization and increases interfacial adhesion between the immiscible polymers. Therefore, investigation of the polymer−polymer interface in such blends has been a long-standing academic and technological challenge.[3−18]

Transmission electron microscopy (TEM) and atomic force microscopy (AFM) are two important techniques for characterization of the interfacial morphology. With TEM, the interfacial thickness and emulsified region can be measured by examining the cross section of the interface.[14−23] With AFM, the roughened interface resulting from compatibilization can be observed by investigation of the revealed surface after removing the top layer.[16−18,21−24] Forward recoil spectrometry (FRES),[6,22,25] secondary ion mass spectrometry (SIMS),[7,26] and time-resolved ellipsometry[19,27] are other important techniques for investigating the interfacial thickness and distribution of the copolymers at the interfacial regions. Although these techniques provide quantitative measurements at the interfacial regions, staining and deuterium labeling are usually necessary for contrast, limiting the types of model polymers available for testing. For some polymer pairs such as polyolefin/nylon and polyolefin elastomer/nylon, the double-staining technique is necessary to deeply stain the interface to get better contrast.[19] Sample preparation, as well as the experiments themselves, may sometimes be difficult or inconvenient to perform. Thin film geometries do not permit the investigation of compatibilization under typical polymer processing conditions.[25] Most importantly, the above-mentioned techniques never catch mechanical information on the constituting polymers and interfacial regions.

In this work, we used a nanomechanical mapping technique, recently developed by our group,[28−30] to investigate the interface of the polymer blends. Interfacial morphology, width, and mechanical property as well as compatibilization effect can be easily evaluated using the surface modulus map obtained from nanomechanical mapping measurements. A reactive compatibilization blend, polyolefin elastomer (POE)/polyamide (PA6), is selected as a model system.

Uncompatibilized POE/PA6 (80/20) and reactive compatibilized POE grafted maleic anhydride/PA6 (POE-*g*-MA/PA6) (80/20) blends were prepared with a micro twin-screw extruder. The resulting blends were first cut using an ultramicrotome at −120 °C to obtain a flat surface. Nanomechanical mapping measurements were operated in the Force Volume (FV) mode on a MultiMode AFM system with a NanoScope V controller. The obtained force−distance curves were analyzed using a procedure developed in our group.[28] Experimental and analytical procedures are reported in the Supporting Information in detail.

The reactive compatibilization of polyolefin/nylon blends has been widely studied for obtaining high-performance materials. The formation of block or graft copolymer by coupling reaction between anhydride/amine leads to a fine morphology and increases the interfacial adhesion of such immiscible blends. Figure 1 shows the Young's modulus map of uncompatibilized POE/PA6 and reactive compatibilized POE-*g*-MA/PA6 blends. The round and blue particles show higher Young's modulus is assigned to the disperse phase PA6 component, while the red areas show lower modulus is assigned to the POE or grafting POE component. The Young's modulus calculated via force−deformation curves (Figure 2a,b) is 2.9 ± 1.1 GPa for PA6 component and 25.5 ± 10.3 MPa for POE or grafting POE component. The curve-fitting against JKR contact is also superimposed in each case. The results show that JKR analysis of the withdrawing process is fitted well for elastic PA6 component. However, deviation appears for the viscoelastic POE component because of the viscoelastic effect. The Young's modulus of both PA6 and POE components agrees well with bulk modulus (PA6: 2.5 ± 0.9 GPa; POE and POE-*g*-MA: 23.5 ± 11.1 MPa). Thus, we may claim that the nanomechanical mapping technique is successful for identifying the composition in those blends. On the other hand, by comparing the two modulus maps, we may observe that the dispersion and particle size of the dispersed phase PA6 becomes homogeneous and displays a very fine dispersion due to the reactive compatibilization. MA groups in compatibilizer react with amine groups in PA6 to form copolymers, which induces a drastic decrease in interfacial tension and suppression of coalescence between the originally immiscible polymer phases.

To obtain a more complete picture at the interfacial regions, Figure 3 shows the Young's modulus map of the uncompatibilized POE/PA6 and compatibilized POE-*g*-MA/PA6 blends with 500 nm scan size. As shown, the interface between the POE and PA6 in uncompatibilized blend is smooth and flat, whereas for the compatibilized blends the interface becomes quite rough after the same processing. Some parts of the POE domain appear to have pinched off at the interface and moved into the PA6. We approximately localize the roughening zone using two dashed lines in Figure 3b. The magnitude of the width of the roughening zone is about 70 nm. A line section across the interface indicated by the white line in Young's modulus map (Figure 3) shows the transition between Young's modulus of the two polymer phases in uncompatibilized blend is sharp while it becomes much wider in the compatibilized blend (Figure 4). We call the transition distance that Young's modulus increases from that of POE to that of PA6 as the interfacial width. The interfacial width for uncompatibilized blend is ∼7.6 nm and, after reactive compatibilization, increases to ∼48 nm. The width of the interface obtained from several line sections from different regions is 9.7 ± 3.6 nm for the uncompatibilized blend and 38.9 ± 19.7 nm for the reactive compatibilized blend. It should be noticed that the occurrence of the interfacial width in the uncompatibilized blend is probably caused by small Flory's interaction parameter (χ)[10,16]

*To whom correspondence should be addressed. E-mail: wangdthu@wpi-aimr.tohoku.ac.jp.

Published on Web 05/28/2010

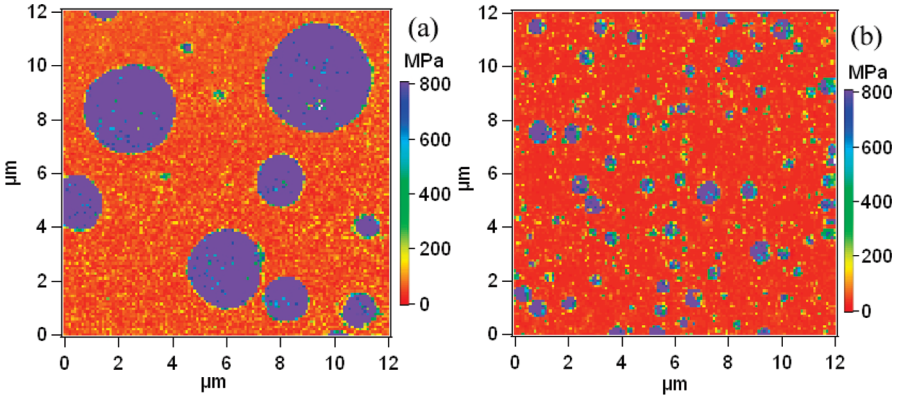

Figure 1. Young's modulus map of (a) uncompatibilized POE/PA6 and reactive compatibilized POE-*g*-MA/PA6 blends. Scan size is 12 μm.

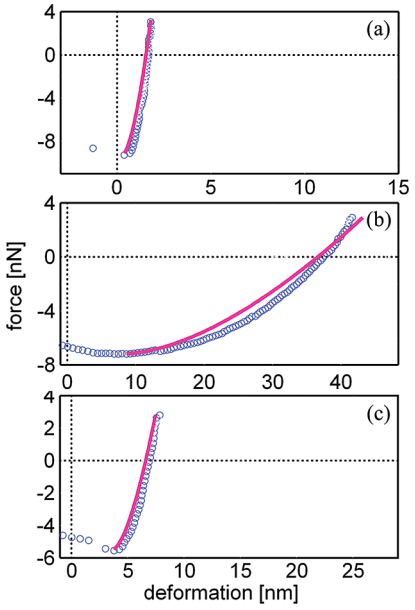

Figure 2. Typical force−deformation curves of (a) PA6, (b) POE, and (c) interfacial regions. The curve fitting against JKR contact was superimposed on each curve. (a) PA6 region, 2.9 ± 1.1 GPa; (b) POE region, 25.5 ± 10.3 MPa; (c) interfacial region, 376 ± 69 MPa.

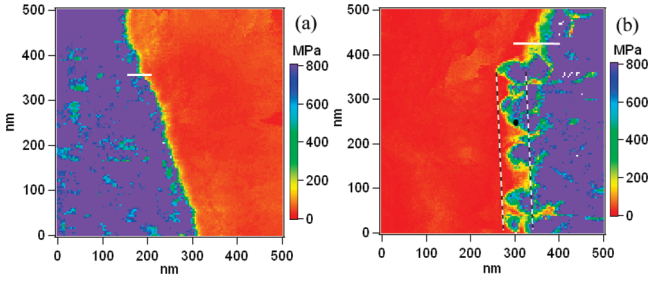

Figure 3. Interfacial roughening observed with nanomechanical mapping: (a) POE/PA6 and (b) POE-*g*-MA/PA6 blends.

or thermal fluctuations,[17,18] but it is much less than that caused by the reactive compatibilization. It is worthy of mention that the interfacial widths reported by Inoue et al.[14,19] and Macosko et al.[17,18] are ~50 nm in polypropylene (PP-*g*-MA)/PA6 or polysulfone (PSU-*g*-MA)/PA6 blends and several hundreds of nanometers in amine-terminal polystyrene (PS-NH_2)/anhydride-terminal poly(methyl methacrylate) (PMMA-anh) blends. It should also be noticed that in the PA6 domain, for both the uncompatibilized and compatibilized blends (Figure 3) as well as

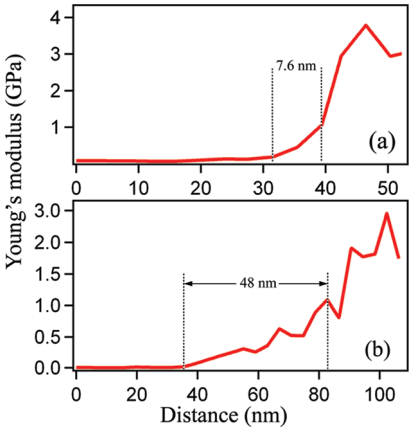

Figure 4. Line section across the interface indicated by the white line in Young's modulus map: (a) POE/PA6 and POE-*g*-MA/PA6 blends.

pure PA6 (Figure 1S), we also observe some light blue area that show Young's modulus 400−700 MPa. The decreased modulus is probably caused by water absorption, which will greatly decrease the mechanical properties of PA6. However, besides measuring the interfacial width, the nanomechanical mapping also enables us to evaluate the interfacial strength. The measured Young's modulus in interfacial regions (indicated by black circle in Figure 3b) is about 375 ± 69 MPa, and its corresponding force−deformation curve is shown in Figure 2c.

In conclusion, nanomechanical mapping has been obtained on a model reactive polymer blend of POE/PA6. This technique enables us not only to measure Young's modulus of the blend components but also to map the morphology of the POE/PA6 blend based on the Young's modulus of the constituting polymers. Furthermore, the most important result is that the interfacial morphology, width, and mechanical property of the blends can be easily evaluated based on the Young's modulus map with several hundreds of nanometers scan size. Comparing these results obtained from nanomechanical mapping with classical characterization methods used for compatibilization, such as TEM, this technique is promising in operation without any staining or coating, and it enables us to directly link the mechanical properties and morphology of the polymer blends. Our results will be useful to study the interfacial reaction and structure of polymer blends as well as composites.

Acknowledgment. The authors thank Prof. Xuming Xie of the Department of Chemical Engineering of Tsinghua University for materials assistance.

Supporting Information Available: Experimental and analytical procedures. This material is available free of charge via the Internet at http://pubs.acs.org.

References and Notes

(1) Paul, D. R.; Bucknall, C. B. *Polymer Blends*; Wiley: New York, 2000.
(2) Koning, C.; Duin, M. V.; Pagnoulle, C.; Jérôme, R. *Prog. Polym. Sci.* **1998**, *23*, 707–57.
(3) Macosko, C. W.; Jeon, H. K.; Hoye, T. R. *Prog. Polym. Sci.* **2005**, *30*, 939–947.
(4) Fredrickson, G. H. *Phys. Rev. Lett.* **1996**, *76*, 3440–3.
(5) Yin, Z.; Koulic, C.; Pagnoulle, C.; Jérôme, R. *Macromolecules* **2001**, *34*, 5132–9.
(6) Schulze, J. S.; Cernohous, J. J.; Hirao, A.; Lodge, T. P.; Macosko, C. W. *Macromolecules* **2000**, *33*, 1191–8.
(7) Harton, S. E.; Stevie, F. A.; Ade, H. *Macromolecules* **2005**, *38*, 3543–6.
(8) Broseta, D.; Fredrickson, G. H.; Helfand, E.; Leibler, L. *Macromolecules* **1990**, *32*, 132–9.
(9) Smith, G. D.; Russell, T. P.; Kulasekere, R.; Ankner, J. F.; Kaiser, H. *Macromolecules* **1996**, *29*, 4120–4.
(10) Russell, T. P.; Menelle, A.; Hamilton, W. A.; Smith, G. S.; Satija, S. K.; Majkrzak, C. F. *Macromolecules* **1991**, *24*, 5721–6.
(11) Guégan, P.; Macosko, C. W.; Ishizone, T.; Hirao, A.; Nakahama, S. *Macromolecules* **1994**, *27*, 4993–7.
(12) O'Shaughnessy, B.; Sawhney, U. *Phys. Rev. Lett.* **1996**, *76*, 3444–7.
(13) O'Shaughnessy, B.; Sawhney, U. *Macromolecules* **1996**, *29*, 7230–9.
(14) Koriyama, H.; Oyama, H. T.; Ougizawa, T.; Inoue, T.; Weber, M.; Koch, E. *Polymer* **1999**, *40*, 6381–93.
(15) Adedeji, A.; Lyu, S.; Macosko, C. W. *Macromolecules* **2001**, *34*, 8663–8.
(16) Kim, H. Y.; Jeong, U.; Kim, J. K. *Macromolecules* **2003**, *36*, 1594–1602.
(17) Zhang, J. B.; Lodge, T. P.; Macosko, C. W. *Macromolecules* **2005**, *38*, 6586–91.
(18) Lyu, S.-P.; Cernohous, J. J.; Bates, F. S.; Macosko, C. W. *Macromolecules* **1999**, *32*, 106–10.
(19) Li, H.; Chiba, T.; Higashida, N.; Yang, Y.; Inoue., T. *Polymer* **1997**, *38*, 3921–5.
(20) Charoensirisomboon, P.; Chiba, T.; Solomko, S. I.; Inoue, T.; Weber, M. *Polymer* **1999**, *40*, 6803–10.
(21) Kho, D. H.; Chae, S. H.; Jeong, U.; Kim, H. Y.; Kim, J. K. *Macromolecules* **2005**, *38*, 3820–7.
(22) Jiao, J. B.; Kramer, E. J.; Vos, S. D.; Möller, M.; Koning, C. *Macromolecules* **1999**, *32*, 6261–9.
(23) Yin, Z.; Koulic, C.; Pagnoulle, C.; Jérôme, R. *Langmuir* **2003**, *19*, 453–7.
(24) Jones, T. D.; Schulze, J.; Macosko, C. W.; Moon, B.; Lodge, T. P. *Macromolecules* **2003**, *36*, 7212–9.
(25) Schulze, J. S.; Moon, B.; Lodge, T. P.; Macosko, C. W. *Macromolecules* **2001**, *34*, 200–5.
(26) Harton, S. E.; Stevie, F. A.; Ade, H. *Macromolecules* **2006**, *39*, 1639–45.
(27) Koriyama, H.; Oyama, H. T.; Ougizawa, T.; Inoue, T.; Weber, M.; Koch, E. *Polymer* **1999**, *40*, 6381–93.
(28) Wang, D.; Fujinami, S.; Nakajima, K.; Nishi, T. *Macromolecules* **2010**, *43*, 3169–72.
(29) Nishi, T.; Nukaga, H.; Fujinami, S.; Nakajima, K. *Chin. J. Polym. Sci.* **2007**, *25*, 35–41.
(30) Nukaga, H.; Fujinami, S.; Watabe, H.; Nakajima, K.; Nishi, T. *Jpn. J. Appl. Phys.* **2005**, *44*, 5425–29.